

Estimation of the global solar radiation using RadEst 3.00 software at Tribhuvan International Airport, Nepal

Nabin Dawadi¹, Manoj Kumar Shrestha², Kisan Khatri³,
Khem Narayan Poudel⁴, Indra Bahadur Karki¹, Babu Ram Tiwari⁴

¹Department of Physics, Patan Multiple Campus, Tribhuvan University, Nepal

²Department of Physics, Amrit Science Campus, Tribhuvan University, Nepal

³Central Department of Physics, Tribhuvan University, Nepal

⁴Department of Applied Science in Chemical Engineering,
IOE Pulchok Campus, Tribhuvan University, Nepal

*Corresponding author. Email: nabindawadi49@gmail.com

Abstract

Daily global solar radiation (GSR) at Tribhuvan International Airport in Kathmandu (27.69° N, 85.35° E; elevation 1338 m) was estimated by using the RadEst 3.0 software, employing meteorological data from 2014 and 2015. The study investigates both seasonal and monthly GSR variations and evaluates overall radiation levels. RadEst 3.0 implements four empirical models: Campbell and Donatelli (CD), Bristow and Campbell (BC), the Modular DCBB model, and Donatelli and Bellocchi (DB), each relying on the diurnal temperature range (the difference in daily peak and low air temperatures) to estimate GSR. The radiation is calculated by multiplying atmospheric transmissivity with extraterrestrial radiation, and the software optimizes model parameters to derive the necessary coefficients. Estimated GSR values and the resulting coefficients were validated against observed data using statistical indicators. Of the models assessed, the Modular DCBB model delivered the most reliable results for the year 2015 with a root mean square error (RMSE) of 2.94 MJ/m², coefficient of determination (R²) of 0.53, residual mass coefficient (CRM) of 0.00, and mean bias error (MBE) of 2.29 MJ/m². These findings identify the Modular DCBB model as the most accurate for the study location and suggest its parameterization is well suited for GSR estimation in regions with similar climatic conditions across Nepal.

Keywords: Global Solar Radiation, Atmospheric Temperature, Precipitation, Coefficient, RadEst 3.00 Software. .

Article information

Manuscript received: July 18, 2025; Revised: October 8, 2025; Accepted: October 9, 2025

DOI <https://doi.org/10.3126/bibechana.v23i1.82026>

This work is licensed under the Creative Commons CC BY-NC License. <https://creativecommons.org/licenses/by-nc/4.0/>

1 Introduction

Nepal lies within the favourable latitudinal range (26° N to 29 °N) and receives substantial solar radiation across its regions. The typical global solar radiation recorded in the country ranges between 3.6 and 6.2 KWh/ m²/day and also experiences sun-

shine for nearly 300days annually, with the mean global solar radiation measured each day around 16.7 MJ/m²/day throughout the year [1].

Meeting the Earth's yearly energy needs would require just around 71 minutes of the solar energy that reaches the planet. Under clear sky conditions, the Earth's surface can receive nearly 1,000 watts

per square meter (W/m^2) of solar irradiance.

Solar radiation tends to increase with altitude under clear and partially cloudy sky conditions; however, on overcast days, the level of solar radiation is significantly lower compared to that on sunny days [2, 3]. The study of solar radiation plays a crucial role in comprehending climate change, assessing environmental pollution, and supporting applications in modern agriculture, the food industry, hydrology, and other developmental programs [4]. Solar resource data is essential for the analysis and optimization of energy systems, ensuring accurate modeling and reliable economic assessments. It provides valuable insights at both local and global scales, informing energy planning and resource management. As a fundamental driver of activities such as cooking, heating, industrial processes, transportation, and lighting, energy underpins economic growth and development. Consequently, ensuring reliable and cost-effective energy supply is essential for advancing sustainable infrastructure and economic resilience [5–7].

To determine the most appropriate model, a comparative evaluation was conducted using RadEst software, which incorporates environmental factors like precipitation and daily atmospheric temperature. Analysis of observed data from 2007 revealed that, among the models assessed, the Modular DCBB model produced the most accurate assessments of global solar radiation (GSR) for the Kathmandu region [1]. Over the past decade, various techniques and strategies have been introduced to compile solar radiation databases using records from meteorological and climatological stations. These approaches often rely on correlation functions, with several models incorporating a broader range of meteorological parameters such as latitude and temperature which are developed through numerous studies [8, 9].

The research on the daily solar radiation in the lowland plains of Nepal by using RadEst 3.00 software was performed, and the global solar radiation was measured. Four different models, namely the Bristow-Campbell model, the Campbell-Donatelli approach, the Bellocchi model, and the Modular DCBB method were utilized to measure global solar radiation by analyzing dynamics of key environmental factors. Various statistical evaluation techniques were employed to evaluate the effectiveness of these models. The results confirmed that the Modular DCBB method provided the highest accuracy in calculating global solar radiation for the study area. It was concluded that the region possesses favorable average global solar radiation levels suitable for energy production and other applications [10].

2 Models

RadEst 3.0 [11, 12] software is a Microsoft Windows-based application (compatible with versions 98, NT, 2000, and XP) designed for estimating total solar radiation of TIA, Kathmandu using meteorological parameters. It estimates and assesses daily global solar radiation at a specified latitude using extreme air temperatures, precipitation, and spatial location. The atmospheric transmissivity is estimated and analyzed by four models using the temperature range between diurnal temperatures. Parameters adopted for these statistical tools are listed below:

tt_i = estimated atmospheric transmissivity

τ = clear sky transmissivity

ΔT = monthly average difference in temperature

T_{max} = daily maximum air temperature

T_{min} = daily minimum air temperature

b = coefficient of temperature range

c = very sensitive empirical parameter

I = day of the year, $I = 1$

T_{nc} = empirical temperature (summer night temperature factor)

c_1 = parameter representing magnitude of seasonal variation

c_2 = parameter describing the profile of seasonal variation

$f(T_{avg})$ = average temperature function

$f(T_{min})$ = minimum temperature function

$EstRad_i$ = estimated solar radiation ($\text{MJ}/\text{m}^2/\text{day}$)

$PotRad_i$ = potential solar radiation outside the Earth's atmosphere ($\text{MJ}/\text{m}^2/\text{day}$)

The estimated radiation value ($EstRad_i$) is calculated by multiplying the estimated transmissivity (tt_i) with the potential solar radiation ($PotRad_i$) received beyond the Earth's atmospheric boundary as,

$$EstRad_i = tt_i PotRad_i$$

The potential radiation ($PotRad_{day}$) is estimated by using the following equation:

$$PotRad_{day} = 117.5 dd2 \{ h_s \sin(lat) \sin(dec) + \cos(lat) \sin(h_s) \} / \pi$$

where latitude of the monitoring site (degrees) is denoted by lat, the solar declination is denoted by dec, the distance between the earth and the sun is

represented by $dd2$, and half- day length (in radians) by h_s . These parameters are calculated using equations below:

$$dd2 = 1 + 0.00334 \cos(0.01721 \text{ day} - 0.00552)$$

$$h_s = \cos^{-1} \{ -\tan(dec) \tan(lat) \}$$

$$dec = \sin^{-1} [0.039785 \sin \{ 4.869 + 0.00172 \text{ day} \\ + 0.003345 \sin(6.224 + 0.00172 \text{ day}) \}]$$

2.1 Bristow and Campbell (BC, 1984) Model

The adopted model is considered as a fundamental approach from which other models have been developed. It is based on the assumption that with reduced atmospheric transmittivity, often caused by increased cloud cover, leads to a decrease in the daily air maximum temperature. Also, this model establishes the correlation between the daily temperature variation and the quantity of sunlight received at the Earth's surface each day.

$$tt_i = \tau \left[1 - \exp \left(\frac{-b\Delta T_i^c}{\text{month}\Delta T} \right) \right]$$

Hence estimated radiation becomes

$$EstRad_i = \tau \left[1 - \exp \left(\frac{-b\Delta T_i^c}{\text{month}\Delta T} \right) \right] PotRad_i$$

where,

$$\Delta T = T_{max_i} - \frac{(T_{min_i} + T_{min_{(i+1)}})}{2}$$

2.2 Campbell and Donatelli (CD, 1998) Model

The proposed model is modified version of the Bristow-Campbell approach, known as CD model, which accounts for situation where night atmospheric temperature cooling is less than the observed on corresponding clear day. The correction factor incorporated from the BC approach into the CD framework allows the latter to account for seasonal effects typical of mid-latitude regions. In this model estimated transmissivity is given as

$$tt_i = \tau [1 - \exp -bf(T_{avg}) \Delta T_i^2 f(T_{min})]$$

Therefore,

$$EstRad_i = \tau [1 - \exp -bf(T_{avg}) \Delta T_i^2 f(T_{min})] PotRad_i$$

where,

$$T_{avg} = \frac{(T_{max_i} + T_{min_i})}{2}$$

2.3 Donatelli and Bellocchi (DB, 2001) Model

DB model calculates radiation based on temperature of air data and, unlike the first two models, integrates the impact of seasonal changes on clear sky transmissivity. This helps in determining c_1 and c_2 its account ΔT using trigonometric function. The transmissivity for this model is given by

$$tt_i = \tau [1 + f(i)] [1 - \exp \{ \frac{-b\Delta T_i^2}{\Delta T_{week}} \}]$$

Giving estimated radiation as

$$EstRad_i = \tau [1 + f(i)] \left[1 - \exp \frac{-b\Delta T_i^2}{\Delta T_{week}} \right] PotRad_i$$

where,

$$f(i) = c_1 \{ \sin(ic_2 \frac{\pi}{180}) + \cos(if(c_2) \frac{\pi}{180}) \},$$

$$f(c_2) = 1 - 1.90c_3 + 3.83c_3^2 \quad \text{and} \quad c_3 = c_2 - \text{interger}(c_2)$$

2.4 Modular DCBB (DCBB, 2003) Model

The fourth model is an inclusive package of all previous models we have known because calculation of radiation in this framework relies on measurements of temperature of air and contains all the character the other three models possess. One can switch the feature manually in specific way, the trigonometric function for several variation and ΔT can be excluded taking $c_1 = 0$ on action.

The atmospheric transmissivity is estimated as,

$$tt_i = \tau [1 + f(i)] \left[1 - \exp \frac{-b\Delta T^2 f(T_{min})}{\Delta T_{avg}} \right]$$

which gives estimated radiation as

$$EstRad_i = \tau [1 + f(i)] \left[1 - \exp \frac{-b\Delta T^2 f(T_{min})}{\Delta T_{avg}} \right] PotRad_i$$

where,

$$f(i) = c_1 \{ \sin(ic_2 \frac{\pi}{180}) + \cos(if(c_2) \frac{\pi}{180}) \},$$

$$f(c_2) = 1 - 1.90c_3 + 3.83c_3^2$$

$$f(T_{avg}) = 0.017 \exp \{ \exp(-0.053 * T_{avg}) \}$$

Here

$$T_{avg} = \frac{T_{max_i} + T_{min_i}}{2}, \wedge f(T_{min}) = \exp(\frac{T_{min}}{T_{nc}})$$

$$c_3 = c_2 - \text{interger}(c_2)$$

3 Methods and Materials

Instrumentation and Data Format: Kathmandu, serving as the capital of Nepal, is located in Province Number 3 at an altitude of roughly 1,350 meters. Within the city, Tribhuvan International Airport (TIA) is positioned at a latitude of 27 degrees 41 minutes 50 seconds north and a longitude of 85 degrees 21 minutes 28 seconds east, with an elevation of about 1,338 meters above mean sea level. This empirical approach utilizes various meteorological data including extreme temperature, rainfall, and solar radiation collected at Tribhuvan International Airport (TIA) in Kathmandu. The dataset covers the years 2014 and 2015 and was obtained from the Department of Hydrology and Meteorology (DHM), Government of Nepal, using a CMP6 pyranometer which is shown in Figure 1, installed at Kathmandu. The most reliable method for obtaining accurate measurements of GSR is the installation of solarimeter or pyranometers at multiple locations as these instruments are suitable for all weather conditions, exhibit low noise levels, and require minimal power for operation. The device remains functional across temperatures from -40°C to 80°C and can detect solar radiation across broad wavelength, ranging between 310 nm - 2800 nm [13, 14].

The thermopile sensor in the instrument is coated with a black surface that efficiently absorbs incoming radiation and convert it into thermal energy. The resulting heat is subsequently transferred to the body of the pyranometer. A voltage signal is generated by the thermopile due to the temperature difference, which corresponds to the intensity of solar radiation [15, 16]. All previously described models require daily meteorological variables such as rainfall, air temperature extremes, and total solar radiation.



Figure 1: CMP6 pyranometer [16].

Specifically, the necessary inputs include day of year (DOY), rainfall in millimeters, T_{\max} and T_{\min} in degrees Celsius, and solar radiation (Rad) expressed in megajoules per square meter per day ($\text{MJ}/\text{m}^2/\text{day}$). The input data must be organized in ASCII files without headers, covering the entire calendar year from day 1 to 365. Using this format, daily global solar radiation was estimated for the years 2014 and 2015 based on observational data collected at Tribhuvan International Airport (TIA), Kathmandu. The parameter fitting process in RadEst 3.00 was carried out using daily sunshine duration, maximum and minimum temperature from the obtained data. The software automatically calibrates model parameters by minimizing the Root Mean Square Error (RMSE) between measured and estimated global solar radiation values. The fitted coefficients for each model were stored in the RadEst parameter archive and then used for model validation and comparison. This ensures that the models are tuned to the local climatic conditions of Kathmandu Valley.

Input Format: Within the RadEst 3.00 software, the initial step involves configuring the geographic parameters, including the altitude, latitude, and longitude of the study site. Users are also required to specify the atmospheric transmissivity under the clear sky condition, generally ranging from 0.60 to 0.80. For all models, this clear sky transmission coefficient is incorporated into the calculation of the atmospheric transmissivity coefficient, whereas the latitude is employed to determine the potential solar radiation.

Analysis: A minimum of two years of data were used, and Auto Optimization (AO) was performed to compare global solar radiation. However, AO proved less accurate than Parameter Fitting (PF) and was excluded from calculations. PF enhances accuracy by accounting for factors that affect solar radiation, simplifying calculations. Parameters such as b , T_{nc} , c_1 , and c_2 were adjusted to match predicted values with measured data. The distinction among the models arises from their respective parameter selections. Data analysis indicated minor discrepancies in measured and observed everyday global solar radiation (GSR), prompting use of statistical metrics to assess their correlation and associated errors. Model accuracy was quantified using four statistical indicators: Mean Bias Error (MBE), Coefficient of Determination (R^2), Coefficient of Residual Mass (CRM), and Root Mean Square Error (RMSE). RMSE was the objective minimized, while MBE, R^2 , and CRM were computed for evaluation only.

4 Results and Discussion

Values of estimated radiation obtained from the auto-optimization method were found to be differ-

ent from those of the measured radiation values. Thus, the daily global solar radiation was calculated using the second approach, which involves fitting parameters. The parameters for each model were adjusted using data from the years 2014 and 2015. The resulting estimates closely corresponded with the observed radiation data. The average radiation measured over the year is $14.5 \text{ MJ/m}^2/\text{day}$. The estimated radiation obtained through Parameter Fitting also matches exactly with the measured value of $14.5 \text{ MJ/m}^2/\text{day}$. Measured radiation peaks at $20.0 \text{ MJ/m}^2/\text{day}$, with a yearly cumulative value of 5300 MJ/m^2 .

Table 1 shows that the annual average radiation estimate calculated by the modular DCBB approach is observed to be closer to the measured annual average radiation than the estimates produced by the other models. So, Modular DCBB model seems to be the best model to estimate the radiation of the year 2014 at TIA, Kathmandu based on measured and estimated value, but the comprehensive evaluation of all models will be conducted through statistical error analysis and correlation parameters.

Table 1: Comparison of Measured, Estimated Average, Maximum, and Annual GSR with Models at TIA, 2014.

Models	Average Value (MJ/m^2)		Maximum Value (MJ/m^2)		Yearly Total (MJ/m^2)	
	MEAS.	EST.	MEAS.	EST.	MEAS.	EST.
BC	14.5	14.5	20.0	25.2	5300	5285
CD	14.5	14.5	20.0	25.9	5300	5275
DB	14.5	14.5	20.0	25.5	5300	5292
MDCBB	14.5	14.5	20.0	22.9	5300	5296

Table 2 presents the maximum, average, and annual total values of estimated and measured global solar radiation (GSR) for 2015, as evaluated using the Parameter Fitting Method. The yearly mean measured solar radiation is 12.6 MJ/m^2 . The estimated radiation obtained through Parameter Fitting also matches exactly with the measured radiation that is $12.6 \text{ MJ/m}^2/\text{day}$. Similarly, maximum value of measured radiation is $22.2 \text{ MJ/m}^2/\text{day}$. The maximum value of estimated radiation obtained by parameter fitting for the models BC, CD, DB, DCBB are 22.2, 24.9, 24.4 and $21.2 \text{ MJ/m}^2/\text{day}$ respectively.

The yearly total solar radiation is $4612 \text{ MJ/m}^2/\text{day}$. From the above Table 2, it is seen that the yearly average value of annual average radiation estimated by the Modular DCBB model is closer to the measured yearly average radiation than the estimates produced by the other models. Thus, considering the comparison between observed and predicted values, the Modular DCBB model appears to be the most accurate for estimating radiation at TIA, Kathmandu in 2015. However, the overall performance of all models will be further assessed using statistical error metrics and correlation parameters.

Table 2: Comparison of Measured, Estimated Average, Maximum, and Annual GSR with Models at TIA, 2015.

Models	Average Value (MJ/m^2)		Maximum Value (MJ/m^2)		Yearly Total (MJ/m^2)	
	MEAS.	EST.	MEAS.	EST.	MEAS.	EST.
BC	12.6	12.6	22.2	22.2	4612	4603
CD	12.6	12.6	22.2	24.9	4612	4601
DB	12.6	12.6	22.2	24.4	4612	4598
MDCBB	12.6	12.6	22.2	21.2	4612	4613

Error Analysis for the Years 2014 and 2015: From the Table 3 and Table 4, we can observe that the RMSE for the Modular DCBB model is less than those calculated for the other models. Thus, the Modular DCBB gives the best model for getting less RMSE in the years 2014 and 2015. All models have estimated values equal with measured value. If we analyze the model evaluated by RadEst 3.0 software in terms of CRM value, all the models have the least CRM value.

Table 3 and Table 4 show that the Mean Bias Error (MBE) for all models is positive for both 2014 and 2015, indicating a tendency toward overestimation. If we analyze the models evaluated by RadEst program in terms of MBE value, we find that the Modular DCBB has the least MBE value, lowest RMSE and highest R^2 . Hence, the Modular DCBB model exhibits the highest accuracy in predicting global solar radiation for the specified study period and location.

Table 3: Error analysis for year 2014

Models	BC	CD	DB	Modular DCBB
RMSE (MJ/m^2)	3.35	3.75	3.39	3.03
MBE (MJ/m^2)	2.65	3.01	2.74	2.36
CRM (no unit)	0.00	0.00	0.00	0.00
R^2 (no unit)	0.43	0.40	0.44	0.48

Table 4: Error analysis for year 2015

Models	BC	CD	DB	Modular DCBB
RMSE (MJ/m^2)	3.11	4.41	34.14	2.94
MBE (MJ/m^2)	2.50	3.81	3.52	2.29
CRM (no unit)	0.00	0.00	0.00	0.00
R^2 (no unit)	0.50	0.27	0.31	0.53

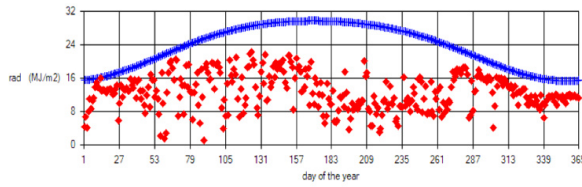


Figure 2: Fluctuation in GSR relative to day of the year 2014.

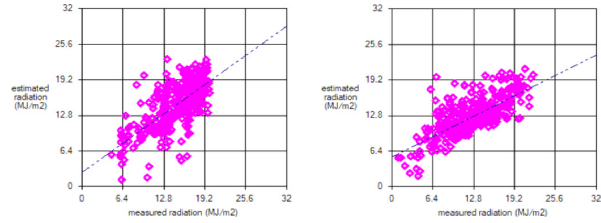
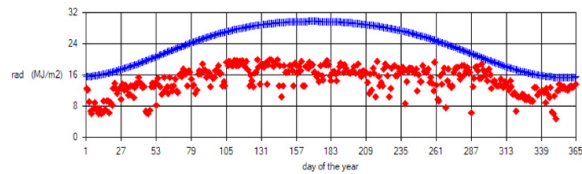
Figure 4: Coefficient of Determination (R^2) between the measured and estimated values of GSR using the DCBB model (Left: 2014, Right: 2015).

Figure 3: Fluctuation in GSR relative to day of the year 2015.

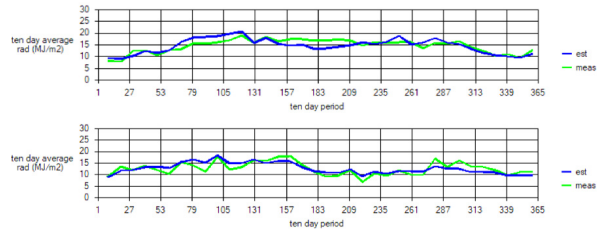


Figure 5: Comparative analysis of ten-day interval averages of measured and estimated GSR for 2014 (top) and 2015 (bottom).

From Figure 2, the peak global solar radiation in 2014 was recorded as $19.96 \text{ MJ}/\text{m}^2/\text{day}$ on day 128, while the minimum was $4.65 \text{ MJ}/\text{m}^2/\text{day}$ on day 350. Similarly, Figure 3 shows that for the year 2015, the maximum global solar radiation reached $22.23 \text{ MJ}/\text{m}^2/\text{day}$ on day 124, and the minimum value was $1.08 \text{ MJ}/\text{m}^2/\text{day}$ on day 89. Figure 4 illustrates that the R^2 values for the years 2014 and 2015 are 0.48 and 0.53, respectively, with the Modular DCBB model achieving the highest R^2 in comparison to the other three models, CD (Campbell-Donatelli), BC (Bristow-Campbell), and DB (Donatelli-Bellocchi).

Presented below are the ten-day averages for both measured and estimated global solar radiation.

Figure 5 illustrates that, during the early part of the year, the estimated GSR values exceed the observed measurements, suggesting possible underestimation in the observed data. In the mid-year period, the measured values surpass the estimates, indicating overestimation, while toward the end of the year, both measured and estimated values converge. These fluctuations can be attributed to several factors, including variations in humidity, aerosol concentrations, and seasonal changes within the Kathmandu Valley.

Table 5 compares our fitted coefficients for TIA, Kathmandu with values reported for other locations. The pattern is similar in both magnitude and trend, showing that our results agree with what others have

found. Based on this, the TIA coefficients can be used as starting values for Nepalese sites with similar weather, with small local adjustments if needed.

Table 5: Model Coefficients for Kathmandu and Selected Other Cities [3, 10, 14].

S.N.	Model	Params	Davis, USA	Padova, Italy	Pretoria, SA	Simara, Nepal	TIA, Kathmandu
1.	BC	B	0.137	0.141	0.126	0.103	0.062
		C	2	2	2	2	2
2.	CD	B	0.262	0.396	0.390	0.153	0.057
		T_{nc}	44.5	42.1	84.8	19.3	11
3.	DB	B	0.122	0.131	0.134	0.095	0.061
		c_1	-0.026	-0.040	-0.053	0.06	-0.1
		c_2	1.410	0.008	0.041	1.045	1.410
4.	DCBB	B	NA	NA	NA	0.081	0.055
		c_1	NA	NA	NA	0.044	0.10
		c_2	NA	NA	NA	0.915	1.410
		T_{nc}	NA	NA	NA	96	106.1

Monthly Fluctuation of Total Solar Radiation at TIA, Kathmandu, 2015: Figure 6 depicts the monthly mean global solar radiation (GSR) values at Tribhuvan International Airport (TIA), Kathmandu, during 2015. The peak GSR of 16.79 MJ/m²/day occurred in May, while the lowest value of 10.88 MJ/m²/day was observed in December. A gradual upward trend in GSR is evident from January to May. However, during the monsoon months of June through September, GSR declines due to persistent cloud cover and overcast conditions. After the monsoon ends in October, GSR rises again, but it subsequently decreases in the remaining months, likely because of atmospheric haze. The months of April, May and June are most favorable months for getting adequate solar radiation. Similarly, December and January are less favorable for the solar radiation and the remaining month received moderate amount of GSR in TIA, Kathmandu.

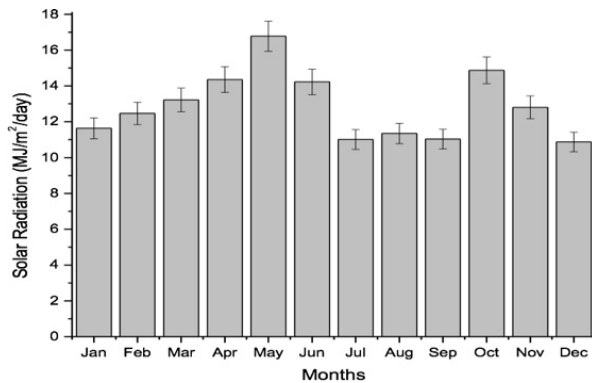


Figure 6: Monthly variations in Global Solar Radiation at TIA, Kathmandu (2015).

GSR Seasonal Changes at TIA, Kathmandu in 2015: Figure 7 illustrates the seasonal fluctuations of global solar radiation (GSR) at Tribhuvan International Airport (TIA), Kathmandu, for

the year 2015. Average GSR values for the spring, winter, autumn, and summer seasons were 14.79, 11.06, 12.90, and 11.19 MJ/m²/day, respectively, with the spring season exhibiting the highest and winter the lowest radiation levels. This occurs because spring has very low rainfall and fewer clouds, leading to continuously increasing sunshine hours and a smaller solar zenith angle. The clear sky conditions during spring allow mostly direct solar radiation, which carries relatively high energy, to reach the Earth's surface. In contrast, high wind speeds, more cloudy days, and increased rainfall during summer reduce global solar radiation.

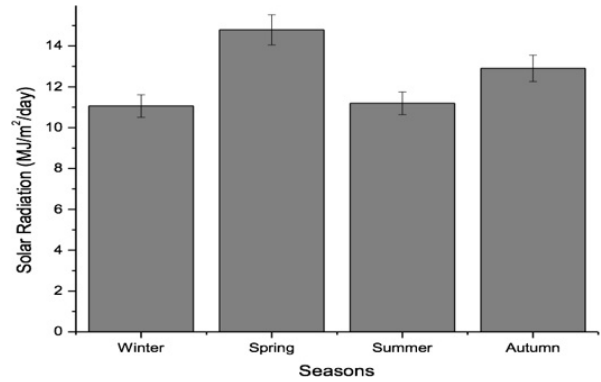


Figure 7: Seasonal changes of GSR at TIA, Kathmandu (2015).

5 Conclusion

Global solar radiation (GSR) measurements at TIA, Kathmandu, were obtained from the CMP6 pyranometer, while GSR estimations were performed using RadEst 3.0 software. Data analysis was done using Origin 8.0, Surfer 13.0, and RadEst 3.0. Yearly and daily averages of GSR for 2014 and 2015 were calculated using parameter fitting and auto optimization for four models. Initially, auto optimization

showed high deviation between measured and estimated values. Parameter Fitting was utilized to calibrate the models, resulting in good consistency among observed and measured values. Seasonal and monthly changes of global solar radiation (GSR) were compared using graphs derived from PF outcomes. The Modular DCBB model performed best, with R^2 values of 0.48 (2014) and 0.53 (2015), and lower RMSE, MBE, and CRM than the other models. Thus, the Modular DCBB model is confirmed as the most accurate for estimating GSR at this location.

However, despite its better performance, the model still produced moderate R^2 values, suggesting that other meteorological variables (e.g., humidity, cloud cover) also influence solar radiation and were not captured. A slight systematic bias was observed during overcast conditions, indicating that the model tends to underestimate solar radiation under such weather patterns. Future work could include longer-term data sets, additional meteorological parameters, adopting hybrid models or machine learning approaches to further improve prediction accuracy.

Acknowledgement

The authors wish to acknowledge the Department of Hydrology and Meteorology (DHM) of the Government of Nepal for their invaluable support in supplying the meteorological data fundamental to this study. They also extend their thanks to the FAO-SDRN Agrometeorology Group based in Rome, Italy, along with ISCI-Crop Science located in Bologna, Italy, for generously providing free access to the RadEst 3.00 software and accompanying user manual through their official online platform.

References

- [1] K. N. Poudyal, B. K. Bhattarai, B. Sapkota, B. Kjeldstad, and P. Daponte. Estimation of the daily global solar radiation; nepal experience. *Measurement*, 46(6):1807–1817, 2013. doi:10.1016/j.measurement.2013.01.012.
- [2] M. Gadiwala, A. Usman, M. Akhtar, K. Jamil, et al. Empirical models for the estimation of global solar radiation with sunshine hours on horizontal surface in various cities of pakistan. *Pakistan Journal of Meteorology*, 9(18):43–49, 2013.
- [3] K. N. Poudyal, B. K. Bhattarai, B. Sapkota, and B. Kjeldstad. Estimation of global solar radiation using sunshine duration in himalaya region. *Research Journal of Chemical Sciences*, 2(11):20–25, 2012.
- [4] M. Iqbal. *An Introduction to Solar Radiation*. Elsevier, 2012.
- [5] J. G. M. Massaquoi. Global solar radiation in sierra leone (west africa). *Solar & Wind Technology*, 5(3):281–283, 1988. doi:10.1016/0741-983X(88)90025-2.
- [6] D. Yakubu and D. W. Medugu. Relationship between the global solar radiation and the sunshine duration in abuja, nigeria. *Ozean Journal of Applied Sciences*, 5(3):221–228, 2012.
- [7] Solargis. Importance of solar resource data for pv system analysis and optimization. <https://kb.solargis.com/docs/data-analysis>, 2024. Solargis Knowledge Base.
- [8] A. Angstrom. Recording solar radiation. *Meddelanden Fran Statens Meteorologisk-Hydrografiska Anstalt*, 3:4–10, 1929.
- [9] K. L. Bristow and G. S. Campbell. On the relationship between incoming solar radiation and daily maximum and minimum temperature. *Agricultural and Forest Meteorology*, 31(2):159–166, 1984. doi:10.1016/0168-1923(84)90017-0.
- [10] K. N. Poudyal, B. K. Bhattarai, B. Sapkota, and B. Kjeldstad. Estimation of the daily global solar radiation using radest 3.00 software—a case study at low land plain region of nepal. *Journal of Nepal Chemical Society*, 29:48–57, 2012. doi:10.3126/jncs.v29i0.9237.
- [11] Research Centre for Industrial Crops. Radest 3.0 [software]. <http://www.isci.it/tools>. No longer available; software downloaded. Accessed on 1 August 2018.
- [12] SIPEAA. Tools. sipeaa – italian society for educational and active learning psychology. <http://www.sipeaa.it/tools>. No longer available. Accessed on 1 August 2018.
- [13] K. N. Poudyal. Estimation of global solar radiation using modified angstrom empirical formula on the basis of meteorological parameters in himalaya region, pokhara, nepal. *Journal of the Institute of Engineering*, 11(1):158–164, 2015.
- [14] M. G. Abraha and M. J. Savage. Comparison of estimates of daily solar radiation from air temperature range for application in crop simulations. *Agricultural and Forest Meteorology*, 148(3):401–416, 2008. doi:10.1016/j.agrformet.2007.10.001.
- [15] J. Awasthi and K. N. Poudyal. Estimation of global solar radiation using empirical model on

- meteorological parameters at simara airport, bara, nepal. *Journal of the Institute of Engineering*, 14(1):143–150, 2018.
- [16] K. N. Poudyal, B. K. Bhattarai, B. K. Sapkota, B. Kjeldstad, and N. R. Karki. Estimation of global solar radiation using pyranometer and nilu-uv irradiance meter at pokhara valley in nepal. *Journal of the Institute of Engineering*, 9(1):69–78, 2013. doi:[10.3126/jie.v9i1.10672](https://doi.org/10.3126/jie.v9i1.10672).